EKF-Based IMU/GPS Sensor Fusion for Robust Urban Vehicle Localization with MPC Path Following

Uchenna C. Onyema, *Member IEEE* and ThankGod A. Njoku

***Abstract*—This paper presents a comprehensive simulation-based study of an Extended Kalman Filter (EKF) framework for fusing Inertial Measurement Unit (IMU) and Global Positioning System (GPS) data to achieve robust vehicle localization in urban driving scenarios. A sixteen-dimensional state vector captures vehicle orientation via quaternions, position, velocity, and sensor biases in a navigation-frame representation. The EKF incorporates nonholonomic motion constraints appropriate for wheeled ground vehicles to improve lateral and vertical velocity estimation. The localization system is evaluated within a closed-loop simulation comprising a high-fidelity 14-Degree-of-Freedom (DOF) Simscape vehicle model, a Model Predictive Control (MPC) path-following controller, virtual IMU and GPS sensor models, and an Unreal Engine visualization interface. Two scenarios are assessed: nominal sensor fusion and GPS signal degradation. Under nominal conditions, the EKF achieves position Root Mean Square Errors (RMSE) of 0.17 m and 0.05 m in the longitudinal and lateral axes, respectively, and attitude RMSEs of 0.17°, 0.2°, and 0.1° in roll, pitch, and yaw. Under GPS degradation, the filter demonstrates graceful performance decay with bounded inertial drift and rapid covariance recovery upon GPS re-acquisition. Throughout all scenarios, the MPC controller remains stable, confirming the suitability of EKF-derived estimates for closed-loop vehicle control.**

***Index Terms*—Extended Kalman Filter, GPS degradation, IMU/GPS integration, Model Predictive Control, nonholonomic constraints, sensor fusion, urban navigation, vehicle localization.**

I. INTRODUCTION

THIS paper presents an Extended Kalman Filter (EKF) framework for fusing Inertial Measurement Unit (IMU) and Global Positioning System (GPS) measurements to achieve robust ground vehicle localization in urban driving environments. Accurate localization is a fundamental requirement for autonomous and advanced driver-assistance systems (ADAS), yet urban settings present severe challenges: GPS signals are regularly degraded by multipath propagation, shadowing, and complete signal blockage caused by tall buildings and infrastructure.

Inertial navigation based on IMU measurements offers high-rate, self-contained estimation but accumulates unbounded drift over time due to sensor noise and bias. GPS provides absolute position corrections but operates at low update rates and is susceptible to environmental degradation. Sensor fusion combining these complementary modalities through a Kalman filter framework has therefore become the de facto approach for practical vehicle navigation.

The EKF is among the most widely adopted techniques for nonlinear state estimation in navigation systems. By propagating uncertainty through a first-order linearization of system dynamics and measurement models, it provides a computationally efficient framework for fusing heterogeneous sensor streams with differing update rates, noise characteristics, and modalities [1].

This paper addresses the tightly coupled interaction between localization and closed-loop model-based control under realistic GPS degradation. The proposed framework integrates: (i) a 16-state quaternion EKF with nonholonomic constraints; (ii) a high-fidelity 14-DOF Simscape vehicle plant; (iii) virtual IMU and GPS sensor models; (iv) an MPC path-following controller; and (v) real-time Unreal Engine visualization. Performance is evaluated over a double lane-change manoeuvre under nominal and GPS-degraded conditions.

II. RELATED WORK

IMU/GPS sensor fusion via Kalman filtering has an extensive research history. Hua et al. [1] demonstrated non-holonomic constrained EKF for real-time GNSS/IMU localization in urban environments, achieving sub-0.5 m accuracy. Zhao et al. [2] proposed adaptive noise estimation for robust IMU/GPS fusion under varying urban conditions. Li et al. [3] developed tightly coupled GNSS/INS integration specifically targeting intermittent GPS availability in urban canyons.

Quaternion-based attitude representations have been widely advocated for navigation filters due to their singularity-free properties [4]. The 16-state formulation—comprising a unit quaternion, position, velocity, gyroscope bias, and accelerometer bias—is consistent with established automotive and aerospace navigation practice.

Model Predictive Control (MPC) has been extensively applied to autonomous vehicle path following [5], [6] owing to its ability to enforce actuator constraints and optimize control effort over a receding horizon. Brossard et al. [7] demonstrated AI-assisted IMU dead-reckoning, while Geneva et al. [8] provided an open-source visual-inertial platform. However, integrated evaluations of EKF estimation quality and MPC

Manuscript received [date to be inserted by IEEE]. This work was carried out At the university of Derby.
Uchenna C. Onyema is with the University of Derby, Derby DE22 1GB, UK (e-mail: onyemauchenna@gmail.com.)
ThankGod A. Njoku is with the University of Derby, Derby DE22 1GB, UK (e-mail: thankgodanjoku@gmail.com).

controller stability under GPS degradation scenarios remain limited in the literature.

III. EKF STATE-SPACE MODEL

A. State Vector Definition

The EKF maintains a 16-dimensional state vector defined as:

$$x = [\, q_0 \;\; q_1 \;\; q_2 \;\; q_3 \;\; b\_gx \;\; b\_gy \;\; b\_gz \;\; p\_N \;\; p\_E \;\; p\_D \;\; v\_N \;\; v\_E \;\; v\_D \;\; b\_ax \;\; b\_ay \;\; b\_az \,]^T \quad (1)$$

where the unit quaternion elements q_0–q_3 parameterize vehicle orientation; $b\_g \in \mathbb{R}^3$ are gyroscope bias states; p_N, p_E, p_D denote position in the North-East-Down (NED) navigation frame; v_N, v_E, v_D are velocity components; and $b\_a \in \mathbb{R}^3$ are accelerometer bias states.

B. Process Model and Predicted State Estimate

The EKF prediction step propagates the state vector forward using raw IMU measurements as control inputs. The nonlinear state transition function is:

$$\hat{x}_k|_{k-1} = f(\hat{x}_{k-1}|_{k-1}, u_k) \quad (2)$$

where $\hat{x}_k|_{k-1}$ is the a priori state estimate and $u_k = [\text{accel}^x, \text{accel}_\gamma, \text{accel}_\varphi, \text{gyro}^x, \text{gyro}_\gamma, \text{gyro}_\varphi]^T$ is the IMU measurement vector. The full component-wise expansion of the predicted state estimate is given in (3):

$$x_{k|k-1} = \begin{bmatrix}
q_0 + \Delta t * q_1(gyrobias_X/2 - gyro_X/2) + \Delta t * q_2 * (gyrobias_Y/2 - gyro_Y/2) + \Delta t * q_3 * (gyrobias_Z/2 - gyro_Z/2) \\
q_1 - \Delta t * q_0(gyrobias_X/2 - gyro_X/2) + \Delta t * q_3 * (gyrobias_Y/2 - gyro_Y/2) - \Delta t * q_2 * (gyrobias_Z/2 - gyro_Z/2) \\
q_2 - \Delta t * q_3(gyrobias_X/2 - gyro_X/2) - \Delta t * q_0 * (gyrobias_Y/2 - gyro_Y/2) + \Delta t * q_1 * (gyrobias_Z/2 - gyro_Z/2) \\
q_3 + \Delta t * q_2(gyrobias_X/2 - gyro_X/2) - \Delta t * q_1 * (gyrobias_Y/2 - gyro_Y/2) - \Delta t * q_0 * (gyrobias_Z/2 - gyro_Z/2) \\
-gryobias_X * (\Delta t * \lambda_{gyro} - 1) \\
-gryobias_Y * (\Delta t * \lambda_{gyro} - 1) \\
-gryobias_Z * (\Delta t * \lambda_{gyro} - 1) \\
position_N + \Delta t * v_N \\
position_E + \Delta t * v_E \\
position_D + \Delta t * v_D \\
v_N + \Delta t * \left\{ \begin{array}{l} q_0 * (q_0 * (accelbias_X - accel_X) - q_3 * (accelbias_Y - accel_Y) + q_2 * (accelbias_Z - accel_Z)) - g_N + \\ q_2 * (q_1 * (accelbias_Y - accel_Y) - q_2 * (accelbias_X - accel_X) + q_0 * (accelbias_Z - accel_Z)) + \\ q_1 * (q_1 * (accelbias_X - accel_X) + q_2 * (accelbias_Y - accel_Y) + q_3 * (accelbias_Z - accel_Z)) - \\ q_3 * (q_3 * (accelbias_X - accel_X) + q_0 * (accelbias_Y - accel_Y) - q_1 * (accelbias_Z - accel_Z)) \end{array} \right\} \\
v_E + \Delta t * \left\{ \begin{array}{l} q_0 * (q_3 * (accelbias_X - accel_X) + q_0 * (accelbias_Y - accel_Y) - q_1 * (accelbias_Z - accel_Z)) - g_E - \\ q_1 * (q_1 * (accelbias_Y - accel_Y) - q_2 * (accelbias_X - accel_X) + q_0 * (accelbias_Z - accel_Z)) + \\ q_2 * (q_1 * (accelbias_X - accel_X) + q_2 * (accelbias_Y - accel_Y) + q_3 * (accelbias_Z - accel_Z)) + \\ q_3 * (q_0 * (accelbias_X - accel_X) - q_3 * (accelbias_Y - accel_Y) + q_2 * (accelbias_Z - accel_Z)) \end{array} \right\} \\
v_D + \Delta t * \left\{ \begin{array}{l} q_0 * (q_1 * (accelbias_Y - accel_Y) - q_2 * (accelbias_X - accel_X) + q_0 * (accelbias_Z - accel_Z)) - g_D + \\ q_1 * (q_3 * (accelbias_X - accel_X) + q_0 * (accelbias_Y - accel_Y) - q_1 * (accelbias_Z - accel_Z)) - \\ q_2 * (q_0 * (accelbias_X - accel_X) - q_3 * (accelbias_Y - accel_Y) + q_2 * (accelbias_Z - accel_Z)) + \\ q_3 * (q_1 * (accelbias_X - accel_X) + q_2 * (accelbias_Y - accel_Y) + q_3 * (accelbias_Z - accel_Z)) \end{array} \right\} \\
-accelbias_X * (\Delta t * \lambda_{accel} - 1) \\
-accelbias_Y * (\Delta t * \lambda_{accel} - 1) \\
-accelbias_Z * (\Delta t * \lambda_{accel} - 1)
\end{bmatrix} \quad (3)$$

The quaternion rows (1–4) encode first-order attitude integration driven by bias-corrected gyroscope measurements. Position rows (8–10) advance by $\Delta t \cdot v$. Velocity rows (11–13) integrate the quaternion-rotated specific force with gravity compensation. Bias rows (5–7 and 14–16) decay according to Gauss–Markov time constants λ_gyro and λ_accel respectively.

The predicted error covariance propagates as:

$$P_k|_{k-1} = F_k \, P_{k-1}|_{k-1} \, F_k^T + Q \quad (4)$$

where F_k is the state transition Jacobian from first-order linearization of $f(\cdot)$, and Q is the process noise covariance matrix encoding accelerometer and gyroscope noise spectral densities and bias random-walk processes.

C. Measurement Update

When GPS measurements are available, the EKF performs a measurement update. The observation model is:

$$z_k = h(\hat{x}_k|_{k-1}) + v_k \quad (5)$$

where $h(\cdot)$ extracts position and velocity components from the state vector, and $v_k \sim \mathcal{C}(0, R)$ is zero-mean Gaussian measurement noise. The Kalman gain is:

$$K_k = P_k|_{k-1} \, H_k^T \, (H_k \, P_k|_{k-1} \, H_k^T + R)^{-1} \quad (6)$$

The a posteriori state and covariance updates are:

$$\hat{x}_k|_k = \hat{x}_k|_{k-1} + K_k \, (z_k - h(\hat{x}_k|_{k-1})) \quad (7)$$

$$P_k|_k = (I - K_k \, H_k) \, P_k|_{k-1} \quad (8)$$

D. Nonholonomic Constraints

For a wheeled ground vehicle, lateral side-slip and vertical velocity are physically constrained under normal operating conditions. Nonholonomic pseudo-measurements enforce these constraints as additional measurement equations within the EKF update step, improving lateral and vertical velocity estimation without additional physical sensors. The constraint measurement noise covariance is a key tuning parameter balancing enforcement strength against tolerance for physical wheel slip.

E. Filter Tuning

Tuning involves selecting Q, R, and the nonholonomic constraint covariance. Q is set according to IMU noise spectral densities and bias instability specifications. R reflects GPS horizontal and vertical position accuracy (HorizontalPositionAccuracy, VerticalPositionAccuracy) and velocity accuracy (VelocityAccuracy). Iterative tuning was performed to achieve consistent covariance behaviour and minimal RMSE under nominal conditions.

IV. SIMULATION ARCHITECTURE

A. Overview

The simulation is implemented in MATLAB/Simulink and integrates four principal subsystems: (1) a high-fidelity 14-DOF vehicle plant; (2) virtual IMU and GPS sensor models; (3) the EKF estimator; and (4) an MPC path-following controller. Unreal Engine is coupled via MATLAB's co-simulation interface for 3D visualization. Ground-truth signals are corrupted by virtual sensor models and fed to the EKF, whose estimates drive the MPC controller, closing the feedback loop. The overall system schematic is shown in Fig. 1, and the corresponding Simulink block diagram is shown in Fig. 2.

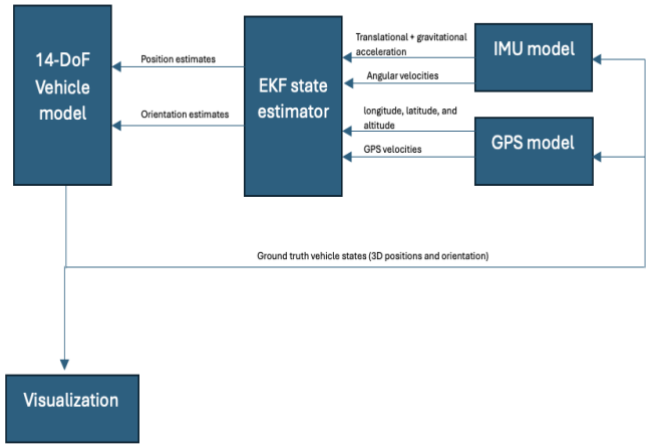

Fig. 1. EKF model schematic illustrating the closed-loop integration of sensor models, state estimator, MPC controller, and vehicle plant.

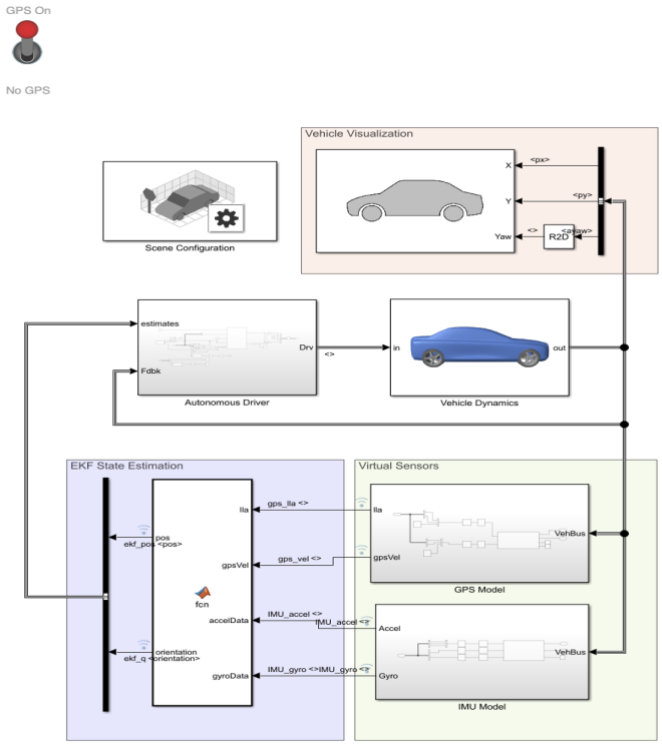

Fig. 2. EKF design block diagram in MATLAB/Simulink showing signal flow between subsystems.

B. IMU Sensor Model

The IMU is modelled using the MATLAB imuSensor System object in an 'accel-gyro' configuration, operating in the NED frame convention. It produces specific force (m/s^2) and angular velocity (rad/s) at a high sampling rate (100–400 Hz), consistent with automotive-grade MEMS devices. Sensor characteristics are parameterized by noise density and bias instability specifications, which are reflected directly in the EKF process noise covariance Q.

C. GPS Sensor Model

The GPS receiver is modelled using the MATLAB gpsSensor System object, generating NED-frame position measurements at 1–10 Hz. Position noise follows a first-order Gauss–Markov process, controlled via HorizontalPositionAccuracy and VerticalPositionAccuracy properties. Velocity noise is additive Gaussian with standard deviation set via VelocityAccuracy. GPS degradation is simulated by increasing noise variance and introducing configurable measurement outages, representative of urban canyon environments.

D. MPC Path-Following Controller

The MPC controller minimizes a quadratic cost penalizing lateral deviation from a reference trajectory, heading error, and control effort, subject to actuator constraints. The optimization is solved over a finite prediction horizon at each control step using the current EKF state estimate. Only the first element of the optimal sequence is applied (receding horizon), and the EKF estimates are transformed into path-relative coordinates (lateral displacement, heading error) for the MPC state vector.

E. 14-DOF Vehicle Model

The vehicle plant is implemented as a 14-DOF model in Simscape Multibody and Simscape Driveline, capturing: longitudinal, lateral, and vertical body translational dynamics; roll, pitch, and yaw sprung-mass dynamics; individual wheel rotational dynamics; nonlinear tire forces; suspension kinematics; and steering system dynamics. This plant provides a demanding simulation environment exercising the full bandwidth of the EKF estimator. The MPC uses a simplified linearized internal model for real-time solvability.

F. Unreal Engine Visualization

Vehicle trajectory and dynamics are rendered in a photorealistic urban environment via MATLAB's Unreal Engine co-simulation interface (Fig. 3). This qualitative visualization complements quantitative RMSE metrics by enabling inspection of trajectory tracking performance, inertial drift onset during GPS outages, and filter recovery behaviour.

Fig. 3. Unreal Engine rendering of the simulated urban driving scenario used for qualitative trajectory visualization.

V. RESULTS AND DISCUSSION

The EKF-MPC system is evaluated over a double lane-change manoeuvre under two conditions: (i) nominal IMU–GPS sensor fusion and (ii) GPS signal degradation active from $t \approx 4$ s to $t \approx 6$ s. Performance is assessed via RMSE, estimation error time histories, and error covariance evolution.

A. Nominal Sensor Fusion

With GPS continuously available, the EKF-estimated trajectory closely follows the ground-truth path. After an initial convergence transient (≈2 s), the filter achieves:

- Position RMSE: 0.17 m (longitudinal), 0.05 m (lateral)
- Attitude RMSE: 0.17° (roll), 0.2° (pitch), 0.1° (yaw)

Fig. 4 shows the vehicle trajectory under nominal fusion. The EKF estimate closely follows the ground truth throughout the lane change. Minor deviations during rapid lateral transitions arise from the update-rate mismatch between high-frequency IMU propagation and lower-frequency GPS corrections but are rapidly attenuated as GPS measurements are incorporated.

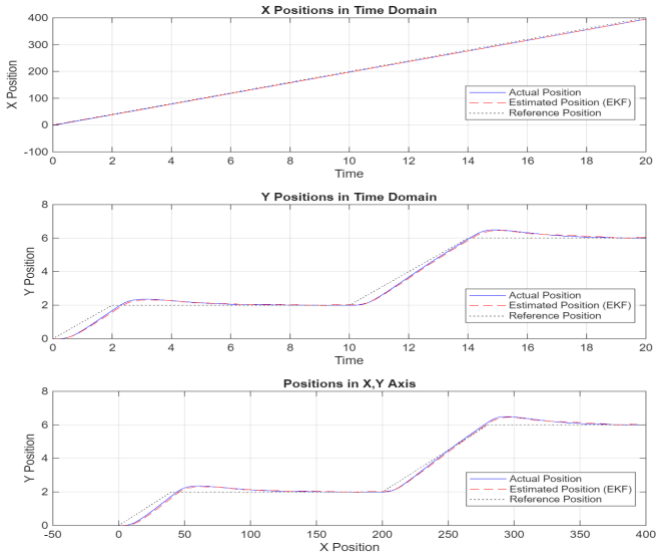

Fig. 4. Position estimation under nominal IMU–GPS sensor fusion during the double lane-change manoeuvre.

Fig. 5 shows the orientation (roll, pitch, yaw) estimates. Roll accurately reflects lateral acceleration during cornering; yaw tracks heading transitions; pitch remains near zero as expected for on-road driving. The smooth signals confirm reliable gyroscope integration and effective bias estimation.

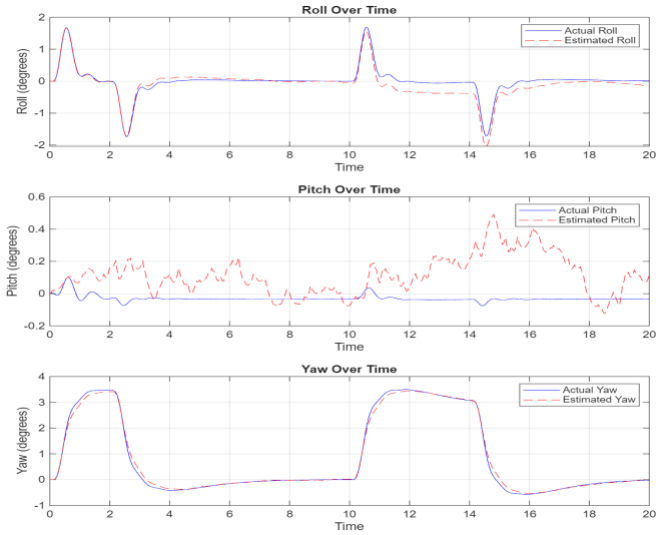

Fig. 5. Orientation (roll, pitch, yaw) estimation under nominal sensor fusion.

Fig. 6 presents position and angle estimation errors over time. Errors remain centred around zero throughout the simulation, with bounded oscillations during the lane change manoeuvre. The bounded nature confirms stable EKF performance and appropriate noise tuning.

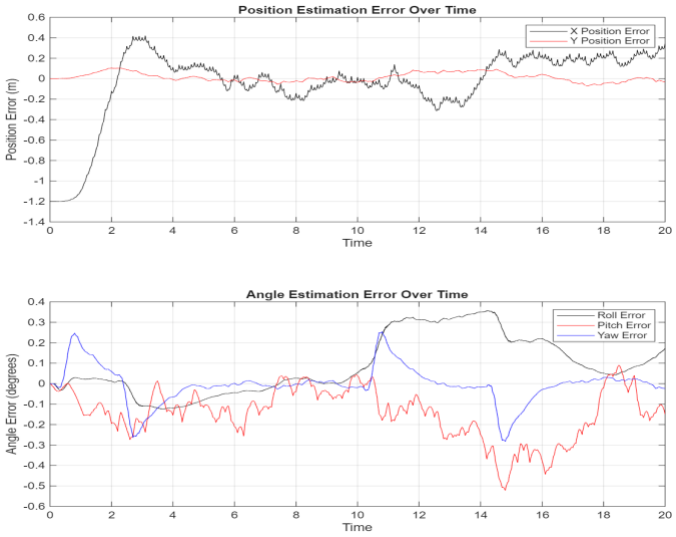

Fig. 6. Position and angle estimation error over time under nominal sensor fusion.

Fig. 7 presents the estimated position error covariance in the x and y channels. After an initial transient reflecting filter convergence, the covariance settles to a low, stable value. This steady-state behaviour confirms that GPS information rate is sufficient to offset IMU propagation uncertainty, yielding a high-confidence state estimate for the MPC controller.

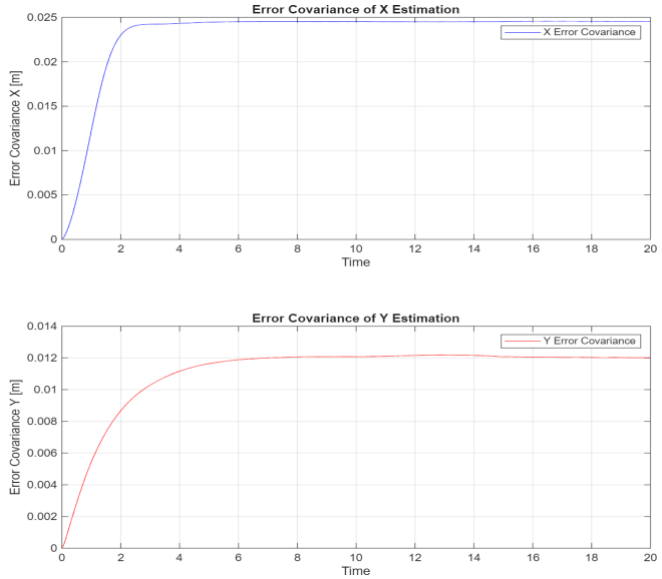

Fig. 7. Estimated position error covariance (x and y channels) under nominal sensor fusion.

B. GPS Signal Degradation

GPS degradation is introduced from t ≈ 4 s to t ≈ 6 s. During this interval the EKF relies on IMU propagation and

nonholonomic constraints to maintain state estimates. Fig. 8 shows the resulting trajectory.

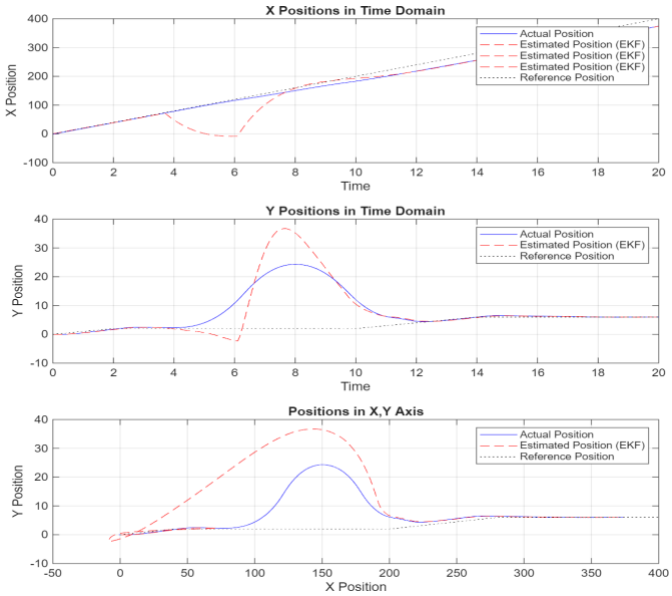

Fig. 8. Position estimation during the GPS degradation interval (active from t ≈ 4 s to t ≈ 6 s).

A gradual divergence between the EKF estimate and ground truth is observed during the outage, characteristic of inertial drift from accelerometer noise integration and bias accumulation in the absence of absolute corrections. Critically, the deviation remains smooth and bounded: the EKF prediction model remains stable and the nonholonomic constraints suppress physically implausible lateral drift. Orientation estimates (Fig. 9) remain well-behaved throughout, as gyroscope-based attitude propagation is less susceptible to short-term drift.

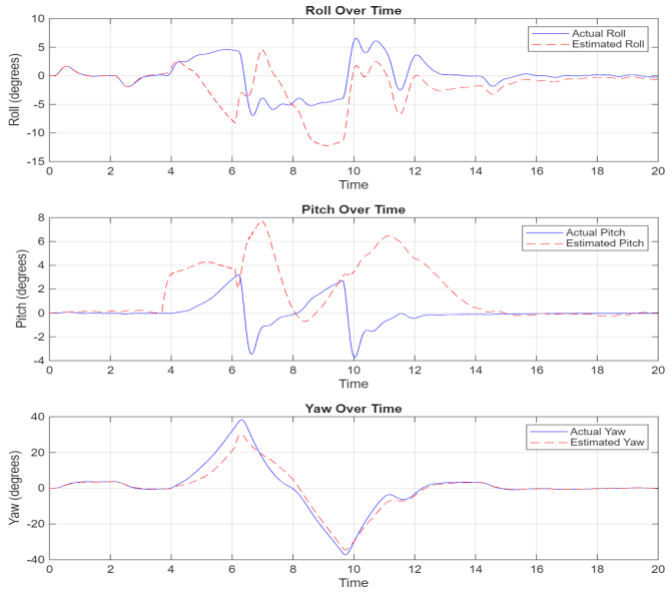

Fig. 9. Orientation estimation during the GPS signal degradation scenario.

Fig. 10 presents the estimation error during GPS degradation. Position error increases steadily in the horizontal plane during the outage, reflecting the loss of absolute corrections. Upon signal recovery at t ≈ 6 s, a sharp error reduction is observed as the EKF measurement update re-aligns the state with GPS measurements.

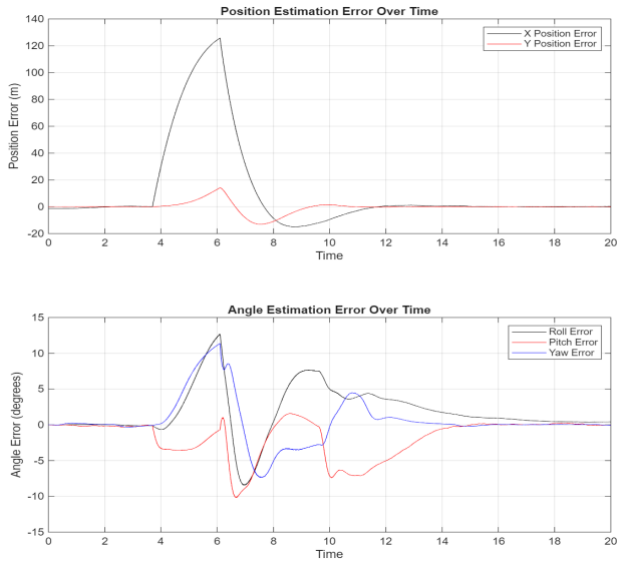

Fig. 10. Position and angle estimation error during the GPS signal degradation scenario.

Fig. 11 shows the estimated error covariance during degradation. The covariance grows markedly during the GPS-denied interval, correctly reflecting growing uncertainty as measurement observability decreases — a key indicator of filter consistency. Upon GPS recovery, covariance decreases rapidly and the trajectory converges back to ground truth.

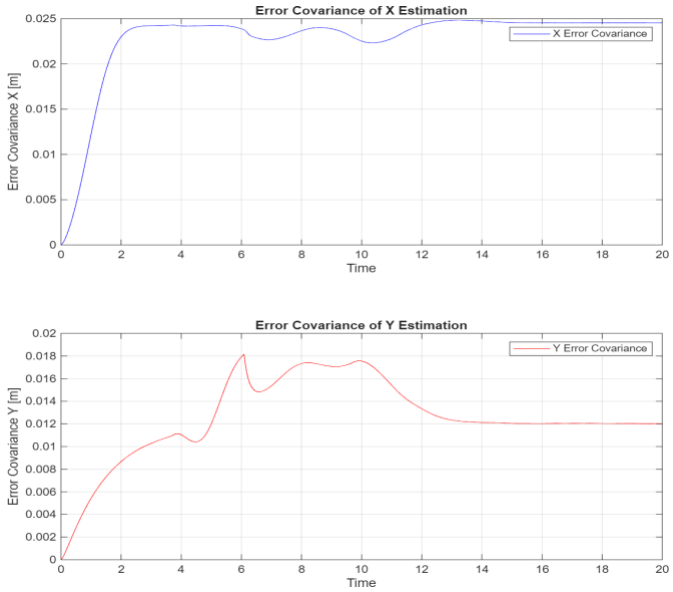

Fig. 11. Estimated position error covariance (x and y) during the GPS degradation scenario.

Despite degraded localization accuracy, the MPC controller continues to track the reference path without instability throughout the GPS outage. This demonstrates the practical benefit of integrating EKF-based estimation with MPC: bounded, consistent state estimates maintain controller stability even under temporary sensor loss.

C. Discussion

The results demonstrate three key properties of the proposed framework: (i) accuracy — sub-0.2 m position RMSE under nominal conditions; (ii) robustness — bounded inertial drift and stable MPC operation during GPS denial; and (iii) consistency — appropriate covariance growth and rapid recovery. Nonholonomic constraints play a discernible role in limiting lateral drift during GPS-denied intervals. The quaternion state representation ensures singularity-free attitude estimation throughout the full yaw range of the manoeuvre.

VI. CONCLUSION

This paper presented and evaluated an EKF-based sensor fusion framework for urban vehicle localization, integrating IMU and GPS measurements within a 16-state quaternion formulation augmented with nonholonomic constraints. The system was embedded in a closed-loop simulation comprising a 14-DOF Simscape vehicle plant, an MPC path-following controller, virtual sensor models, and Unreal Engine visualization.

Simulation results across nominal and GPS-degraded double lane-change manoeuvres demonstrated accurate and consistent state estimation, with nominal position RMSEs of 0.17 m and 0.05 m in the longitudinal and lateral axes, stable inertial-only operation during GPS outages, and rapid covariance recovery upon signal re-acquisition. The MPC controller remained stable throughout all scenarios, confirming the suitability of EKF estimates for closed-loop vehicle control.

Future work will investigate additional sensor modalities (wheel odometry, vision-based localization), incorporation of estimation uncertainty into a robust MPC formulation, and real-world experimental validation on an instrumented ground vehicle platform.

REFERENCES

[1] T. Hua, H. Liu, T. Chen, N. Li, and H. Wang, "High accuracy non-holonomic constrained EKF for real-time GNSS/IMU-based vehicle localization in urban environments," IEEE Access, vol. 9, pp. 24159–24168, 2021, doi: 10.1109/ACCESS.2021.3056088.

[2] S. Zhao, H. Chen, and F. Farooq, "Robust vehicle localization via IMU/GPS sensor fusion with adaptive noise estimation," IEEE Trans. Intell. Transp. Syst., vol. 24, no. 3, pp. 3042–3054, Mar. 2023, doi: 10.1109/TITS.2022.3216412.

[3] X. Li, Y. Ge, H. Su, J. Li, and R. Fang, "Tightly coupled GNSS/INS integration for urban vehicle navigation with GPS signal intermittency," GPS Solutions, vol. 27, no. 2, p. 88, 2023, doi: 10.1007/s10291-023-01425-x.

[4] A. Barrau and S. Bonnabel, "Invariant Kalman filtering," Annu. Rev. Control Robot. Auton. Syst., vol. 1, pp. 237–257, May 2018, doi: 10.1146/annurev-control-060117-105010.

[5] M. Schwenzer, M. Ay, T. Bergs, and D. Abel, "Review on model predictive control: An engineering perspective," Int. J. Adv. Manuf. Technol., vol. 117, pp. 1327–1349, 2021, doi: 10.1007/s00170-021-07682-3.

[6] B. Paden, M. Cap, S. Z. Yong, D. Yershov, and E. Frazzoli, "A survey of motion planning and control techniques for self-driving urban vehicles," IEEE Trans. Intell. Veh., vol. 1, no. 1, pp. 33–55, Mar. 2016, doi: 10.1109/TIV.2016.2578706.

[7] M. Brossard, A. Barrau, and S. Bonnabel, "AI-IMU dead-reckoning," IEEE Trans. Intell. Veh., vol. 5, no. 4, pp. 585–595, Dec. 2020, doi: 10.1109/TIV.2020.2980758.

[8] P. Geneva, K. Eckenhoff, W. Lee, Y. Yang, and G. Huang, "OpenVINS: A research platform for visual-inertial estimation," in Proc. IEEE Int. Conf. Robot. Autom. (ICRA), 2020, pp. 4666–4672, doi: 10.1109/ICRA40945.2020.9196524.

[9] J. Huang, X. Zeng, Z. Wan, and M. Yi, "Nonholonomic constraints aided tightly coupled GNSS/INS integrated navigation for ground vehicle," IEEE Access, vol. 11, pp. 15515–15526, 2023, doi: 10.1109/ACCESS.2023.3244963.

[10] Y. Zhang, J. Liu, and Z. Lian, "Adaptive extended Kalman filter for GNSS/INS integrated navigation under time-varying noise conditions," IET Radar Sonar Navig., vol. 17, no. 5, pp. 831–844, May 2023, doi: 10.1049/rsn2.12382.

[11] P. Falcone, F. Borrelli, J. Asgari, H. E. Tseng, and D. Hrovat, "Predictive active steering control for autonomous vehicle systems," IEEE Trans. Control Syst. Technol., vol. 15, no. 3, pp. 566–580, May 2007, doi: 10.1109/TCST.2007.894653.

[12] MathWorks, "Vehicle Dynamics Blockset — 14-DOF vehicle model," 2024. [Online]. Available: https://www.mathworks.com/help/vdynblks/

[13] MathWorks, "Unreal Engine Visualization — Automated Driving Toolbox," 2024. [Online]. Available: https://www.mathworks.com/help/driving/

Uchenna C. Onyema (Member, IEEE) is a recent PhD graduate of the University of Derby. He holds a background in Electronic Engineering and a master's degree (Distinction, 2018) from the University of Derby. He has accumulated experience collaborating with national research centers, contributing to cross-disciplinary projects at the intersection of academia and industry, teaching engineering core disciplines as an Associate Lecturer. His current research interests include advanced control systems, renewable energy, autonomous localization, and the application of machine/deep learning to complex engineering problems. Mr. Onyema is an active Member of IEEE and IET UK and a recipient of multiple awards for academic and research impact.

ThankGod A. Njoku is a researcher with a background in Electronics and Computing and a master's degree in information systems from the University of Bedfordshire. He has built his career at the intersection of innovation and enterprise, actively working on developing technology-driven solutions through startup ventures.

His work focuses on applying cutting-edge research to real-world challenges, particularly within the domains of blockchain, machine learning, smart government systems, and advanced control systems. ThankGod is currently leading the development of a startup that leverages these technologies to create scalable and impactful solutions.

His research interests center on integrating emerging technologies into practical applications, with a strong emphasis on innovation, efficiency, and digital transformation across industries.